



## EXPERIMENTAL TESTS OF A GROIN VAULT IN DRY-BONDED VOUSOIRS UNDER DYNAMIC EXCITATION

D. Foti<sup>(1)</sup>, S. Silvestri<sup>(2)</sup>, S. Baraccani<sup>(3)</sup>, S. Ivorra<sup>(4)</sup>, D. Theodossopoulos<sup>(5)</sup>, V. Vacca<sup>(6)</sup>, V. Campanella<sup>(7)</sup>, J.V. Ochoa Roman<sup>(8)</sup>, L. Cavallini<sup>(9)</sup>, R. White<sup>(10)</sup>, M. Dietz<sup>(11)</sup>, G. Mylonakis<sup>(12)</sup>

<sup>(1)</sup> Full Professor, Technical University of Bari, Italy, [dora.foti@poliba.it](mailto:dora.foti@poliba.it)

<sup>(2)</sup> Associate Professor, University of Bologna, Italy, [stefano.silvestri@unibo.it](mailto:stefano.silvestri@unibo.it)

<sup>(3)</sup> Research Fellow, University of Bologna, Italy, [simonetta.baraccani2@unibo.it](mailto:simonetta.baraccani2@unibo.it)

<sup>(4)</sup> Full Professor, University of Alicante, Spain, [sivorra@ua.es](mailto:sivorra@ua.es)

<sup>(5)</sup> Lecturer, University of Edinburgh, UK, [dtheodo1@exseed.ed.ac.uk](mailto:dtheodo1@exseed.ed.ac.uk)

<sup>(6)</sup> Research Fellow, Technical University of Bari, Italy, [vitantonio.vacca@poliba.it](mailto:vitantonio.vacca@poliba.it)

<sup>(7)</sup> Civil Engineering, Tecnocontrolli S.r.l., Italy, [enzocamp30@gmail.com](mailto:enzocamp30@gmail.com)

<sup>(8)</sup> Graduate Student, University of Bologna, Italy, [jacqueline.ochoa@studio.unibo.it](mailto:jacqueline.ochoa@studio.unibo.it)

<sup>(9)</sup> Graduate Student, University of Bologna, Italy, [luca.cavallini10@studio.unibo.it](mailto:luca.cavallini10@studio.unibo.it)

<sup>(10)</sup> Research Associate, University of Bristol, UK, [rory.white@bristol.ac.uk](mailto:rory.white@bristol.ac.uk)

<sup>(11)</sup> Research Fellow, University of Bristol, UK, [M.Dietz@bristol.ac.uk](mailto:M.Dietz@bristol.ac.uk)

<sup>(12)</sup> Full Professor, University of Bristol, UK, [G.Mylonakis@bristol.ac.uk](mailto:G.Mylonakis@bristol.ac.uk)

### Abstract

The work at hand presents an experimental study of the dynamic and earthquake response of a groin vault carried out at the EQUALS shaking table, University of Bristol, under the auspices of SERA/H2020 project. The vault considers dry joints between the voussoirs (like many monumental structures in South Mediterranean) and was built in an innovative way to allow study of its dynamic behaviour and repetition of tests carried out until collapse. To the best of the authors' knowledge, no investigations of this kind have been carried out in the past.

The physical model was generated by the intersection of two circular barrel vaults, without ribs but with especially shaped blocks along the groins. Each block was manufactured with a 3D printed skin and filled with mortar to supply mass. The skin was made with a plastic material to provide the blocks with sufficient stiffness and strength to sustain impact without damage and allow for a quick and reliable re-assembly.

The vault was tested on the 3m x 3m, 6-dof shaking table at the University of Bristol, U.K.. Harmonic and transient earthquake motions were imposed in one horizontal direction with increasing amplitude, up to collapse.

Preliminary results showed that low frequencies (around 2Hz and 5 Hz at model scale) are critical. It was noticed that the barrel vault perpendicular to the motion deflected significantly around the key-stone line, eventually leading to collapse.

**Keywords:** groin vault; shaking table test; 3D printed blocks; frequencies; SEBESMOVA3D.



## 1. Introduction

An efficient structural form of historical vaults is made of voussoirs (stone, brick) that support each other through normal pressure on their contact faces. A common type of masonry vault is the cross vault, which results from the intersection of two barrel vaults at right angles [1]. When the semi-cylinders intersect with some inclination, the structure takes the name of raised cross or groin vault (Fig. 1).

Vaults are a very common type of ceiling in historical buildings. Notable collapses have been observed during earthquakes. Some examples are shown in Fig. 2 [2, 3, 4]. From what has been observed in many failures, it is their central portions that collapse and not their supports, as they are embedded into the latter while they counteract the outward thrust of the roof system.

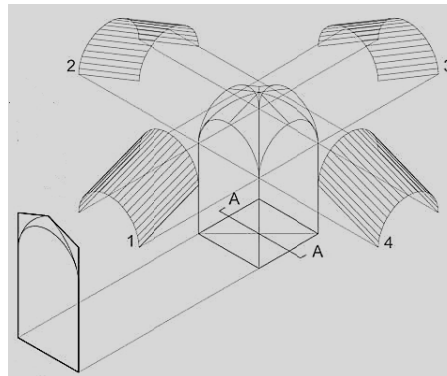
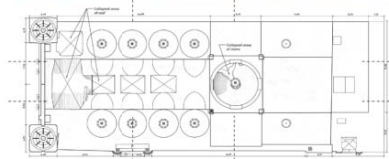


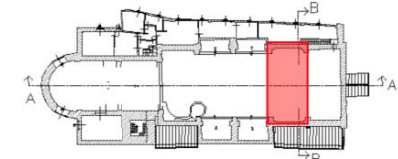
Fig. 1 – Groin vault.



Cathedral of Ica  
Ica, Peru  
2007



Basilica di San Francesco d'Assisi  
Perugia, Italy  
1997



Chiesa di San Pietro in Oliveto  
Brescia, Italy  
2004

Fig. 2 – Examples of collapses of vaults in historical churches.

This paper presents some results of a wide experimental campaign funded by SERA/Horizon2020 that aimed at developing know-how on the seismic behaviour of groin vaults through a comprehensive set of shaking-table tests carried out at the EQUALS Laboratory, University of Bristol, on a properly scaled model [5]. This physical model was realised with dry-joint blocks made of a 3D-printed plastic skin filled with mortar, which provided sufficient stiffness and strength to sustain impact without damage and allow for a quick and reliable re-assembly. This technique was used in similar tests previously performed on a small barrel vault at the “Laboratorio Salvati”, Technical University of Bari (Italy) [6]: the arches and vaults tested were made with modular blocks of wood and stone, respectively, and assembled with dry joints [7,8].



The main objective of the SERA project named “SEismic BEhavior of Scaled MOdels of groin VAults made by 3D printers (SEBESMOVA3D)” is to evaluate the crack pattern and collapse mechanism of groin vaults with two different support conditions: four fixed springings (Configuration 1) and two fixed springings combined with two moveable points characterized by very low lateral stiffness (Configuration 2). The rationale behind this choice lies in the observation that a vault under earthquake excitation is mainly subjected to two different phenomena: (i) response of the vault to differential horizontal shear displacement imposed at its springings by the excitation of the underlying structures (walls and piers, characterised by different lateral stiffness) [9], and (ii) dynamic response of the vault itself to acceleration imposed at its springings. The information to be gained from the effect of the supporting structures is fundamental to correctly plan seismic strengthening intervention projects in vaults and will be useful to professional engineers.

The experimental campaign was carried out in two separate sessions: August 2019 and January/February 2020. In this paper, only the first session is presented which focused on Configuration 1. Harmonic and transient earthquake motions were imposed in one horizontal direction with increasing amplitude, up to collapse.

## 2. Design phase of the vault model

### 2.1 Geometrical configuration

The physical model was designed as an assembly of distinct plastic-mortar blocks (Fig. 3). A plastic mould formed the blocks, made by a 3D printer, which was then filled up with mortar to acquire the corresponding mass for dynamic tests [5]. The assemblage of the blocks was assisted with a polystyrene formwork, to ensure the model would be efficiently and quickly rebuilt after each collapse. In addition, to ensure a fixity condition at the base, 2-cm-thick steel plates were attached to the shakingtable to prevent the four springing blocks to move in translation. The global dimensions of the vault were adjusted to fit the facilities of the EQUALS laboratory at University of Bristol, leading to a large physical model occupying a 2m x 2m area [10]. The model was truncated at the base to encompass the effect of the base embedded in any supporting element, as observed in the vault collapses surveys briefly mentioned in the Introduction (Fig. 4).

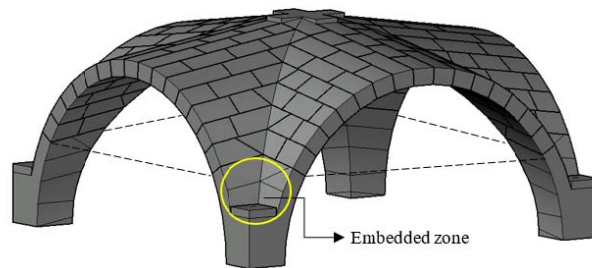


Fig. 3– Original design of the vault (before truncating the base).

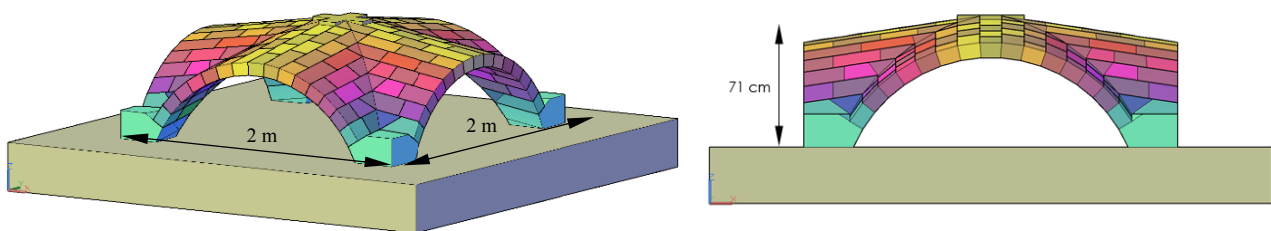


Fig. 4 – Final design of the vault, truncated at the base to account for the connection with perimeter walls and stiff springings.



The thickness of the truncated vault is 8 cm and its height is approximately 71 cm. It is composed by 172 blocks, five of them having larger dimensions than the others: the four bases on which the structure is set up (Fig. 5) and the keystone (Fig. 6), which locks all the pieces into position. The dimensions of a typical block are 12 cm x 8 cm x 20 cm (Fig. 7).

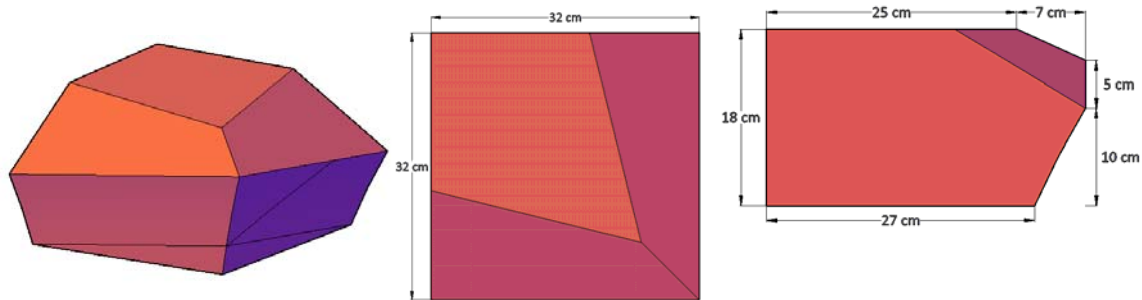


Fig. 5 – Shape and dimensions of the blocks at the base.

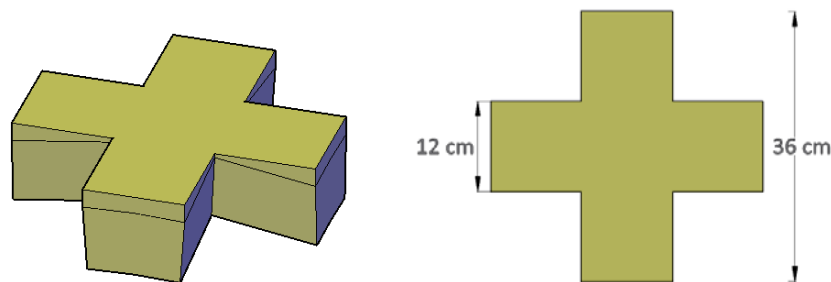


Fig. 6 – Shape and dimensions of the keystone.



Fig. 7 – Typical blocks.

## 2.2 Materials

The composite blocks of the vault are fastened to each other with a gum layer to increase frictional and dissipative properties and allow for small adjustments during construction, since no fresh mortar is used between the bricks.

Simple trials were carried out to establish the best interface solution and provide a high friction angle (Fig. 8). Three contact cases were considered: (1) plastic–plastic, (2) plastic–gum layer–plastic, (3) plastic–double gum layer–plastic. The third solution was selected to achieve the least possible slippage.

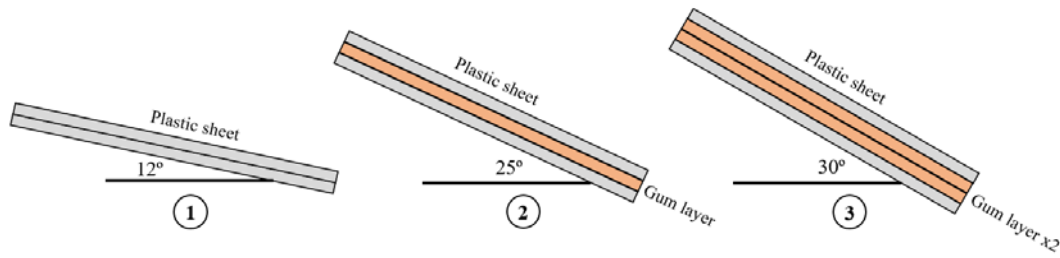


Fig. 8 – Friction angle trials.

The material to fill the blocks is Thistle bonding coat from British Gypsum. To assess the mechanical properties of this infill mortar, a compression test of a cylindrical sample hardened in similar conditions was carried out (Fig. 9): the elastic modulus was estimated as  $E = 60 \text{ N/mm}^2$  and compression strength was  $0.25 \text{ N/mm}^2$ .

Likewise, the mechanical properties of the mortar-skin-gum set were assessed via cyclic compression tests of a single brick filled with mortar and gum-layer around (Fig. 10). The initial part of the first cycle provides information about the gum layer's elastic modulus ( $E = 0.8 \div 1.0 \text{ N/mm}^2$ ) as this is the first element of the set that is compressed. The subsequent part of the first cycle returns an elastic modulus for the block of  $40 \text{ N/mm}^2$ , which is mostly provided by the stiffness of the plastic skin box. For higher forces, mortar starts working. It is also important to note that during motion, and especially for high accelerations (e.g., Peak Table Acceleration - PTA), the effective Young modulus of the vault continuously changes in time and space, as detachments between the bricks may occur in various places. On the average, the effective Young's modulus of the vault as considered as made of an equivalent elastic material turned out to be mainly governed by that of the gum layer.

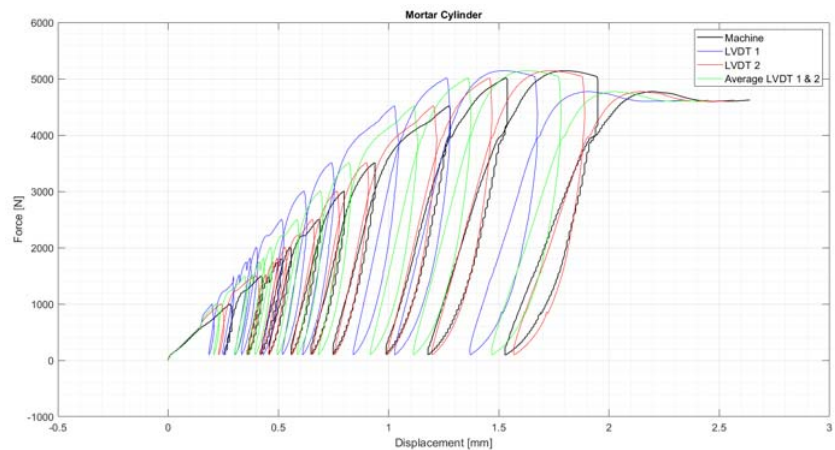


Fig. 9 – Force-displacement diagram for the mortar cylinder.

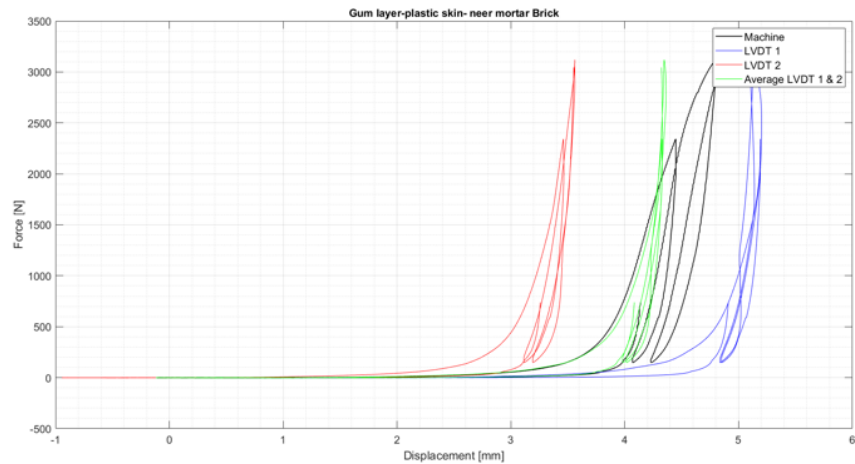


Fig. 10 – Force-displacement diagram for a sample brick, filled with mortar and gum-layer around.

### 3. Construction phases

The plastic brick moulds were pre-assembled to verify dimensions, shapes and number of units, as shown in Fig. 11. Then, the vault was dismantled to fill up the units with mortar.

The steel plates were fixed on the shaking-table (Fig. 12). First, the base blocks were installed followed by the other bricks placed on the polystyrene formwork starting from the lateral arches; once the first row of blocks in every lateral arch was completed, the diagonal blocks were installed, followed by the other blocks of the webs (Fig. 13).

The final assembly on the shaking table was completed successfully (Fig. 14) and once the formwork was removed, as expected, due to the flexibility provided by the gum layers and the lack of lateral confinement especially in the springing areas (typically expected in actual masonry vaults), the vault could not withstand its own weight, i.e. it failed statically (as expected - Fig. 14).

Lateral confinement therefore became necessary and was provided by four 2 cm-thick wooden panels installed along the lateral arches (Fig. 15) **Errore. L'origine riferimento non è stata trovata.** The initial actual configuration with respect to the theoretical one is shown in Fig. 16. The keystone moved vertically 6.6 cm due to the adjustments provoked by the compression of the gum layers. The shape was designed to have an approximate inclination of 7.7%, while the actual inclination is around 5.5%.



Fig. 11 - Pre-assembly of the plastic skin of the blocks.

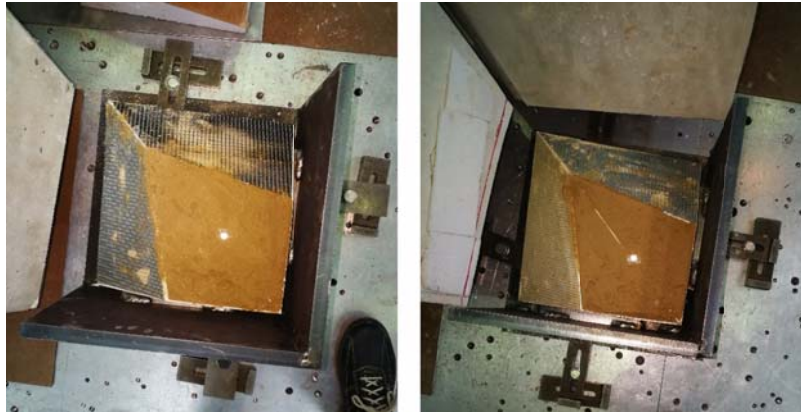


Fig. 12 - Steel plates on the corners to fix the base.



Fig. 13 – Assembly process.



Fig. 14 - Physical model before the formwork removal and afterwards, showing the failure mechanism under gravity load.



Fig. 15 - Wooden panels installed to provide confinement.

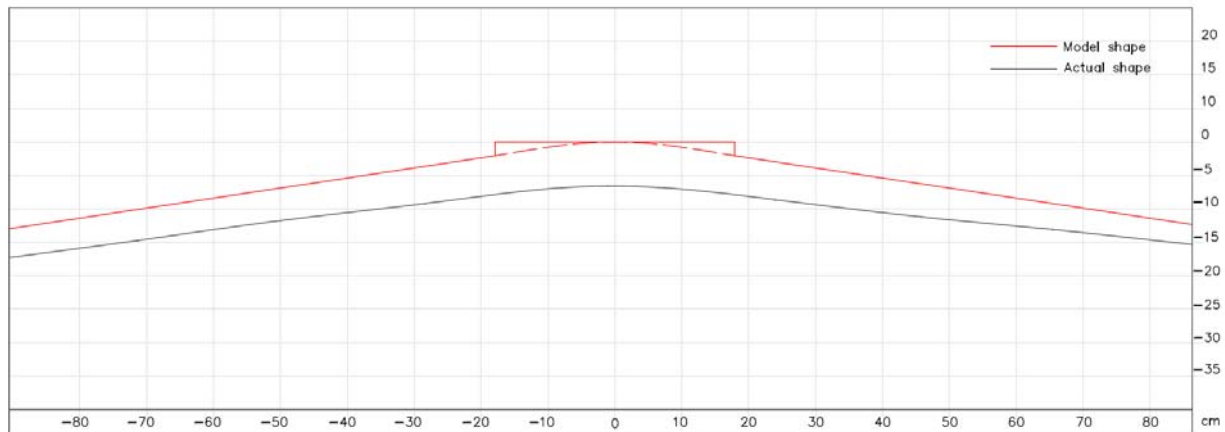


Fig. 16 - Actual and designed central arch's shape.

## 4. Experimental tests

### 4.1 Test set-up and instrumentation

The test rig consists of: (a) a 3m x 3m shaking table platform which can carry up to 15 tons of payload and can reach accelerations up to about 5g with peak displacements of  $\pm 150$ mm; (b) a data Acquisition System that includes a 250-channel system and an advanced wireless system based on 8 high definition digital cameras; (c) markers that are placed atop each block to measure displacements [6]; (d) triaxial accelerometers on the shaking table (Fig. 17a) and on the keystone of the vault operating at a frequency rate of 5000 Hz; (e) a vision system composed by motion capture cameras recording the positions during time of the markers placed on each brick (Fig. 17b) at a frequency rate of 100 Hz.

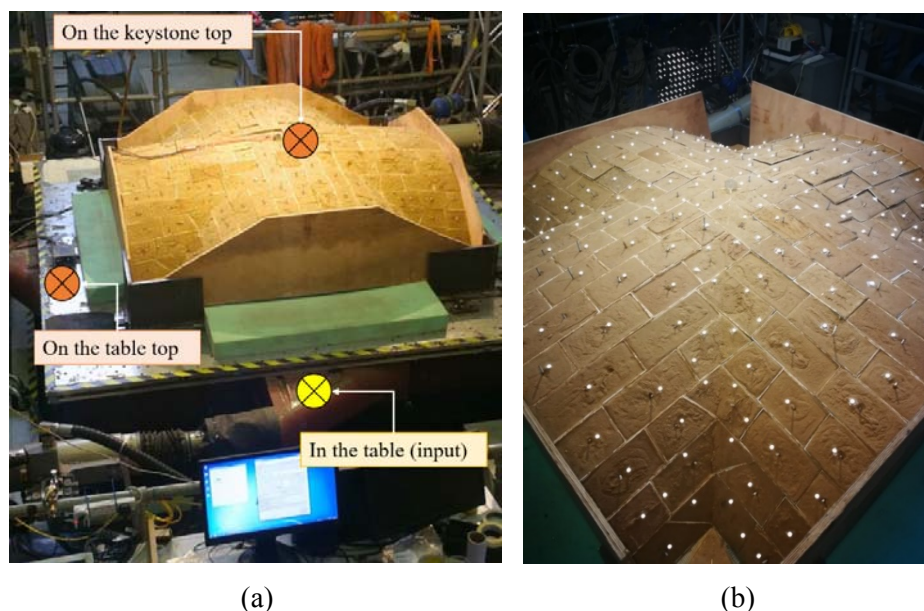


Fig. 17 – (a) Position of the triaxial accelerometers. (b) Position of the markers.

### 4.2 Testing program

The experimental campaign was carried out in two separate sessions: August 2019 and January/February 2020. In this paper, only the first session is presented which was developed in three stages (Table 1), each of them was a series of consecutive tests with reconstruction only after collapse, i.e. each test accumulated the damage of the preceding ones.



Table 1 – List of tests.

Test	Description		Test	Description	
1	'White noise test - x direction'		32	'white noise test - x-direction'	
2	'White noise test - y direction'		33	'harmonic test - x-direction 0.8g, 15Hz'	0.80g
3	'White noise test - z direction'		34	'harmonic test - x-direction 0.8g, 10Hz'	
4	'harmonic test - x-direction: 0.1g, 1Hz'	0.10g	35	'harmonic test - x-direction 0.8g, 8Hz'	
5	'harmonic test - x-direction: 0.1g, 5Hz'				
6	'harmonic test - x-direction: 0.1g, 8Hz'				
7	'harmonic test - x-direction: 0.1g, 10Hz'				
8	'harmonic test - x-direction: 0.1g, 15Hz'				
9	'harmonic test - x-direction: 0.1g, 20Hz'	0.25g	36	'harmonic test - x-direction 0.8g, 5Hz'	
10	'harmonic test - x-direction: 0.1g, 50Hz'				
11	'harmonic test - x-direction: 0.25g, 1Hz'				
12	'harmonic test - x-direction: 0.25g, 5Hz'				
13	'harmonic test - x-direction: 0.25g, 8Hz'				
14	'harmonic test - x-direction: 0.25g, 10Hz'	0.50g	37	'harmonic test - x-direction 0.8g, 2Hz'	
15	'harmonic test - x-direction: 0.25g, 15Hz'				
16	'harmonic test - x-direction: 0.25g, 20Hz'				
17	'harmonic test - x-direction: 0.25g, 50Hz'				
18	'harmonic test - x-direction: 0.50g, 1Hz'				
19	'harmonic test - x-direction: 0.50g, 5Hz'	0.75g	38	'harmonic test - x-direction 0.85g, 15Hz'	
20	'harmonic test - x-direction: 0.50g, 8Hz'				
21	'harmonic test - x-direction: 0.50g, 10Hz'				
22	'harmonic test - x-direction: 0.50g, 15Hz'				
23	'harmonic test - x-direction: 0.50g, 20Hz'				
24	'harmonic test - x-direction: 0.50g, 50Hz'	0.90g	39	'harmonic test - x-direction 0.85g, 10Hz'	
25	'harmonic test - x-direction: 0.75g, 2Hz'				
26	'harmonic test - x-direction: 0.75g, 5Hz'				
27	'harmonic test - x-direction: 0.75g, 8Hz'				
28	'harmonic test - x-direction: 0.75g, 10Hz'				
29	'harmonic test - x-direction: 0.75g, 15Hz'	0.95g	40	'harmonic test - x-direction 0.85g, 8Hz'	
30	'harmonic test - x-direction: 0.75g, 20Hz'				
31	'harmonic test - x-direction: 1g, 2Hz'		1g	41	'harmonic test - x-direction 0.85g, 5Hz'
				42	'harmonic test - x-direction 0.85g, 2Hz'
				43	'harmonic test - x-direction 0.90g, 15Hz'
			44	'harmonic test - x-direction 0.90g, 10Hz'	
			45	'harmonic test - x-direction 0.90g, 8Hz'	
			46-2	'harmonic test - x-direction 0.90g, 5Hz (repeat)'	
			46	'harmonic test - x-direction 0.90g, 5Hz'	
			47	'harmonic test - x-direction 0.90g, 2Hz'	
			48	'harmonic test - x-direction 0.95g, 15Hz'	
			49	'harmonic test - x-direction 0.95g, 10Hz'	
			50	'harmonic test - x-direction 0.95g, 8Hz'	
			51	'harmonic test - x-direction 0.95g, 5Hz'	
			52	'harmonic test - x-direction 0.95g, 2Hz'	
			53	'white noise test - x-direction'	
			54	'seismic test 1'	
			55	'white noise test - y-direction'	
			56	'seismic test 2'	
			57	'seismic test 3'	
			58	'seismic test 4'	
			59	'seismic test 5'	
			60	'seismic test 6'	
			61	'harmonic test - y-direction, 1g, 5Hz'	
			62	'harmonic test - y-direction, 1.2g, 5Hz'	
			63	'harmonic test - y-direction, 1.4g, 5Hz'	

Harmonic tests with frequencies ranging between 1 Hz and 50 Hz were explored, with special emphasis in the range between 2 Hz and 15 Hz, in which most of the damage is inflicted. Additionally, six tests using actual earthquake motions were carried out. However, no significant damage was observed in the latter tests since the vault seemed to be more vulnerable to harmonic motions of low frequencies. The barrel vault perpendicular to the motion deflected significantly around the key-stone line, eventually leading to collapse. The vault collapsed three times: two at 2 Hz with a PTA of 0.95g and 1g, and one at 5Hz with a PTA of 1.4g. A hinge at the extrados was recorded before total collapse the second time (Fig. 18a), while Fig. 18b shows the partial failure mechanism around the keystone in the third time.

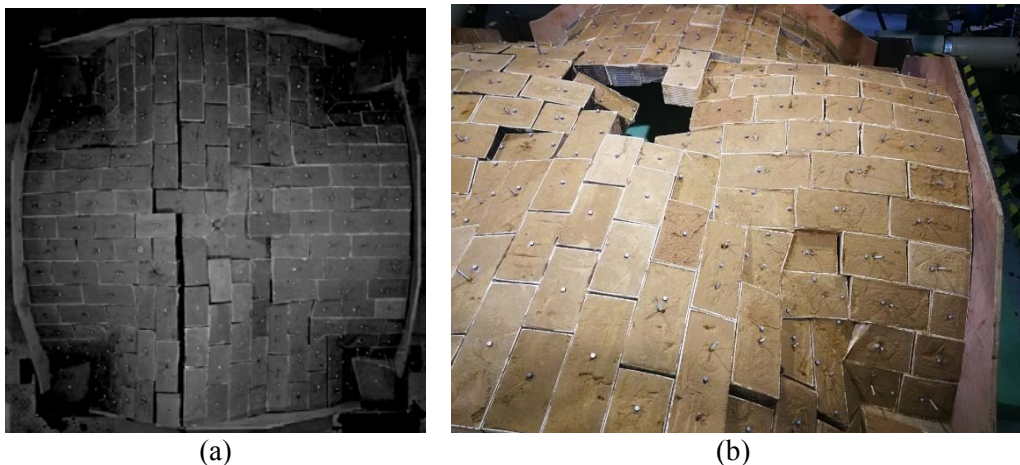


Fig. 18 – Failure mechanism at: (a) 2Hz with PTA of 1.0g, (b) 5Hz with PTA of 1.4g.



### 4.3 Frequencies and key-stone maximum displacements

The physical model was vulnerable to low frequencies, especially near 2Hz, whose maximum induced displacements far exceed the displacements produced by inputs of higher frequencies and same PTA (Fig. 19).

Key-stone maximum relative (with respect to the table) displacements to frequency inputs such as 50Hz, 20Hz or 15Hz exhibit an almost horizontal asymptotic behaviour as the acceleration increases and can be considered small. Inputs with frequencies between 5Hz and 10Hz produced maximum displacements that increase “linearly” with acceleration. Inputs of 2Hz induced large movements (unexpected amplification), which could indicate that the “natural frequency” of the physical model is around that value, at least for large acceleration values ( $>0.8g$ ).

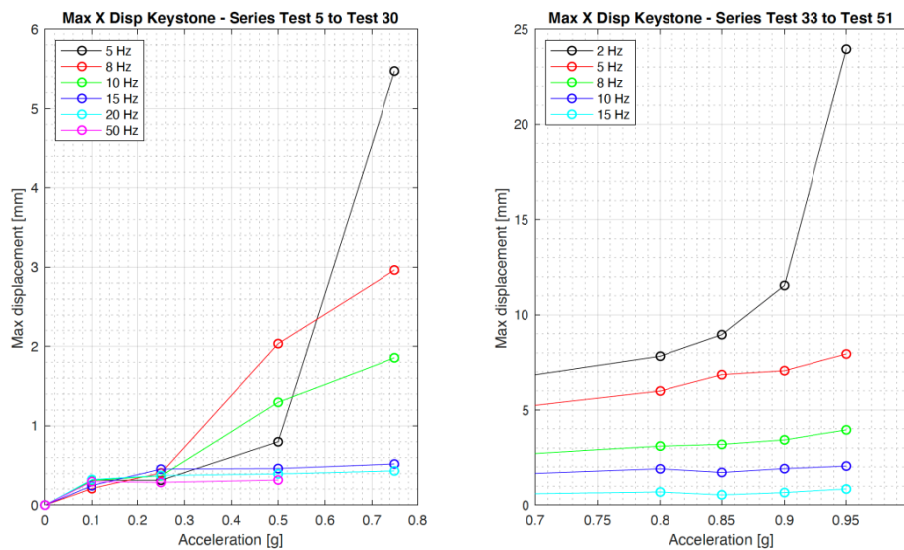


Fig. 19–Maximum displacement of the keystone as function of the Peak Table Acceleration for sinusoidal input characterized by different frequencies (two series of tests).

### 4.4 Damage accumulation

Since no reassembly of blocks was done prior to collapse, each test naturally starts from a displaced configuration that can be interpreted as a “cumulative damage” state. Figures 20 and 21 show the cumulative displacement of the keystone before collapse. In the horizontal direction (X, the one of the applied input), the cumulative displacement before the last test of the first sequence is around 1.5 mm, while in the vertical direction (Z) it is 13.5 mm. For the second sequence, displacements seem to be higher than in the first (i.e., 2.8 mm in the horizontal and 57 mm in the vertical direction, respectively).

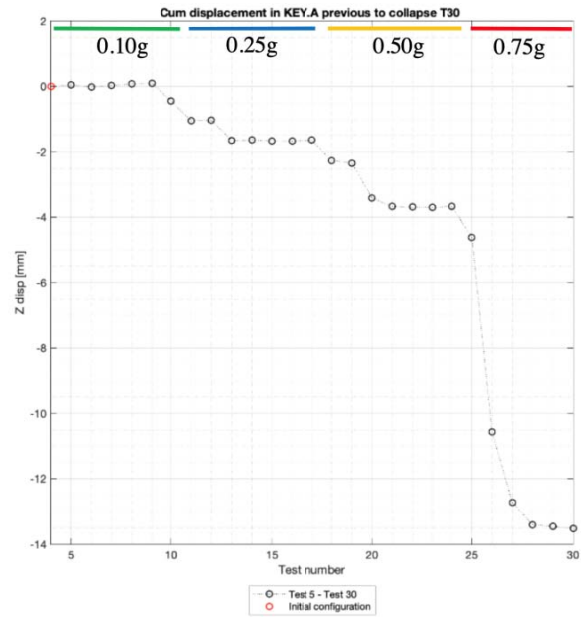
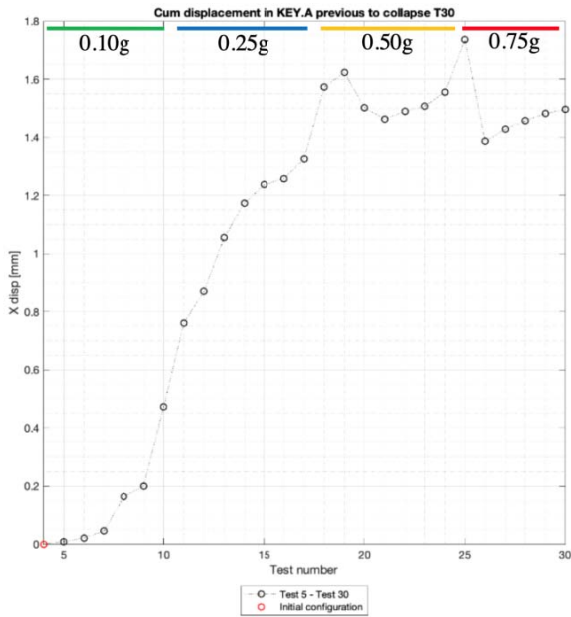


Fig. 20 – Cumulative displacement series T4 – T30 in directions X and Z.

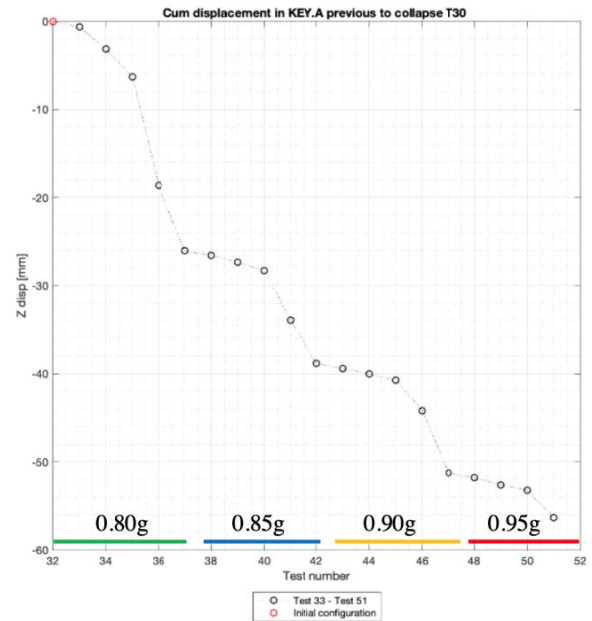
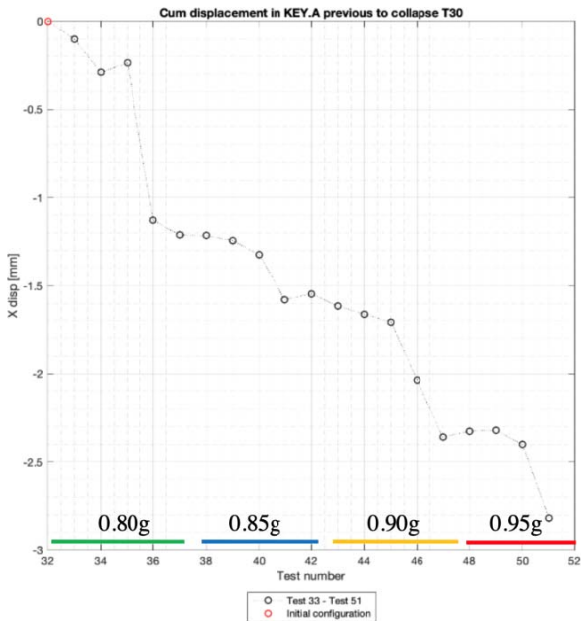


Fig. 21 – Cumulative displacement series T33-T51 in directions X and Z.

### 5. Conclusions

The article at hand reports on a series of shaking table tests performed on a scaled groin vault model made of plastic 3D printed blocks filled with mortar. The advantages of using 3D printers to manufacture the blocks relate to the workability and the repeatability of the tests: the plastic-mortar blocks can be immediately reused after each test as they are fixed with a gum layer, not fresh mortar. Seismic and harmonic inputs, with different frequencies ranging between 1Hz and 50Hz, were imposed in one horizontal direction with increasing amplitude, up to collapse. The springings of the model were fixed on the shaking table to provide the necessary lateral static forces and ensure equilibrium. Cracking patterns corresponding to vertical and horizontal displacements of all bricks and the failure mechanisms were recorded during the tests.



The presence of the gum layer has a strong influence on the global behaviour and seems to govern the dynamic response of the structure, especially for high-acceleration and low frequency inputs. The results of the experimental campaign revealed a tendency to activate different stiffness for each Peak Table Acceleration (PTA) level and each frequency, which indicates a strongly non-linear behaviour.

## Acknowledgements

This project “SEismic BEhavior of Scaled MOdels of groin VAULTs made by 3D printers (SEBESMOVA3D)” has received funding from the European Union’s Horizon 2020 research and innovation programme under Grant Agreement No 730900. The authors would like to thank the personnel of EQUALS Laboratory at University of Bristol, for their help and hospitality during execution of these tests.

## References

- [1] Honour, H., Fleming, J. (2009). *A World History of Art*. 7th edn. London: Laurence King Publishing.
- [2] Croci, G. (1998). *The Collapses Occurred in the Basilica of St Francis of Assisi and in the Cathedral of Noto. Structural Analysis of Historical Constructions II*. Barcelona: CIMNE.
- [3] Piermarini, E. (2013). *The Dynamic Behavior of the Basilica of San Francesco of Assisi*. Master Thesis. Massachusetts Institute of Technology.
- [4] Cancino, C. (2009). *Estudio de daños a edificaciones históricas de tierra después del terremoto del 15 de agosto del 2007 en Pisco, Perú*. The Getty Conservation Institute, Los Angeles: J. Paul Getty Trust 2011.
- [5] Seismology and Earthquake Engineering Research Infrastructure Alliance for Europe. SERA TA Project # 22: *Seismic Behavior of Scaled Models of groin Vaults made by 3D printers*. <https://sera-ta.eucentre.it/index.php/sera-ta-project-22/>. Accessed: 8 Oct 2019.
- [6] Foti, D., Vacca, V., Facchini, I. (2018). DEM modelling and experimental analysis of the static behavior of a dry-joints masonry cross vaults, *Construction and Building Materials*, 170, 111-120.
- [7] Foti, D., Lerna, M., Sabbà, M.F., Vacca, V. (2019). On the collapse behavior of a wood arch made with modular hollow blocks. *WSEAS Transactions on Environment and Development* 15, Article number 31, 279-287.
- [8] Diaferio, M., Dassisti, M., Foti, D., Vacca, V. (2019). Analysis of a Mock-Up of a New Sustainable Easy-Assembling Modular Arch. *Structures*, 19, 309-321.
- [9] Carfagnini, C., Baraccani, S., Silvestri, S., Theodossopoulos, D. (2018). The effects of in-plane shear displacements at the springings of Gothic cross vaults. *Construction and Building Materials*, 186, 219–232.
- [10] Faculty of Engineering, University of Bristol. *Earthquake and Geotechnical equipment and facilities*. <http://www.bris.ac.uk/engineering/research/earthquakegeo/equip/>. Accessed: 8 Oct 2019.